International Journal of
Georesources and Environment
http://ijge.camdemia.ca, ijge@camdemia.ca
IJGE 2018 4(3): 133-140
Available at http://ojs.library.dal.ca/ijge
Research and Development and Industry

Investigation of Effects of Nanobubbles on Phosphate Ore Flotation

Dongping Tao[1]*, Maoming Fan[2], Zhongxia Wu[1], Xuyu Zhang[1], Qianshuai Wang[1], Zekang Li[1]
[1] School of Mining Engineering, University of Science and Technology Liaoning, Anshan, Liaoning, China
[2] Canadian Process Technologies, Inc., Eriez Manufacturing Company, Erie, Pennsylvania, USA

Abstract: Phosphorous is vital for life, including plants, animals, and human beings and it is an essential component in agricultural fertilizers and phosphorous-based chemicals. Phosphate ores, mainly in the form of apatite and collophanite, are non-renewable natural resources of phosphorus. Froth flotation has been used in the phosphate industry for more than half a century as the primary technique for upgrading phosphate. Nevertheless, flotation does not produce satisfactory performance for phosphate beneficiation in many cases, especially for very fine and coarse phosphate particles. This study was performed with an aim to develop a nanobubble enhanced flotation process to enhance phosphate flotation efficiency. A specially designed flotation column featured with a nanobubble generator and a conventional bubble generator was employed to assess the effects of nanobubbles on the phosphate ore flotation performance under different operating conditions. Flotation process parameters investigated include feed flow rate, dosage of collector, dosage of frother, flotation time, etc. The flotation results have shown that use of nanobubbles increased P_2O_5 recovery by up to 30% for a given Acid Insoluble (A.I.) rejection, depending on phosphate concentrate grade. Nanobubbles reduced the collector and frother dosage by about 50% and also increased flotation kinetics. The improved flotation performance can be attributed to increased collection efficiency and surface hydrophobicity in the presence of nanobubbles.

Keywords: attachment, bubble size, cavitation, collision, nanobubble, phosphate

1 Introduction

Phosphate rock often exists in the form of apatite and collophanite and represents a vital non-renewable resource of phosphorous which is vital for life, including plants, animals, and human beings. It is a commodity which is neither substitutable nor recyclable in agricultural applications. The demand for phosphorous must be met through mining, beneficiation, and chemical processing of naturally derived phosphate deposits. China, Morocco, Russia and the United States of America are four leading producers of phosphate rock in the world and their outputs account for 72% of the total annual production of 160 million tons (Van Kauwenbergh 2010). The increased need for world food production assures the long-term growth in world phosphate rock demand. Nevertheless, the run-of-mine phosphate ore is low in P_2O_5 grade, contains high concentrations of impurities such as quartz, chert, clay, feldspar, mica, calcite, and dolomite and thus cannot be used directly to produce commercial products. It requires upgrading or beneficiation to reduce the content of gangue minerals to meet given specifications. For example, in the fertilizer industry the phosphate concentrate must satisfy these required criteria: 1) P_2O_5 content larger than 30%, 2) CaO/P_2O_5 ratio smaller than 1.6, and 3) MgO content less than 1%.

Froth flotation is the most widely used process for phosphate beneficiation where fatty acids are often used as collectors (Sis and Chander 2003). In this process hydrophobic phosphate particles are captured by air bubbles, ascend to the top of the pulp zone, and eventually report to the froth product whereas hydrophilic gangue minerals such as silicates, carbonates, and clays remain in the pulp and are discharged as tailings. Although the most recent studies (Priha et al 2014, Mendes et al 2014, Calle-Castañeda et al 2018) have shown that biological processes may be used for upgrading low grade phosphates, the vast majority of world's marketable phosphate is produced by froth flotation. However, the high separation efficiency of froth flotation is limited to a very narrow particle size range, which is usually 10-100 μm. In fact, one of the most difficult technical challenges facing the mineral processing industry is the recovery of fine (<37 μm) and ultrafine (<8–13 μm) mineral particles by flotation (Calgaroto et al 2015). It is generally believed that the low flotation efficiency of fine particles is primarily due to the low probability of bubble-particle collision while the main reason for poor flotation recovery of coarse particles is the high probability of detachment of particles from bubble surface (Ralston and Dukhin 1999, Yoon 2000, Tao 2004).

Tremendous efforts have been made to improve flotation recovery of phosphate particles. Davis and Hood

* Corresponding Author: Dongping Tao, Email: dptao@qq.com, phone: +86 138 1346 7505

DOI: 10.15273/ijge.2018.03.022

(1993) found that optimized conditioning process improves the recovery. Moudgil (1992) reported that the recovery of phosphate particles can be enhanced by means of collector emulsification, and use of more effective frother, etc. Maksimov et al (1993) reported that weak agitation combined with sufficiently high ascending pulp flow in a mechanic flotation cell substantially increased the flotation recovery of coarse mineral particles. Rodrigues et al (2001) observed that the flotation recovery of coarse particles is strongly affected by hydrodynamic conditions and maximum flotation recovery was achieved when the hydrodynamic parameters were in a certain range. They attributed the low flotation recovery of coarse particles under too quiescent conditions to particle settling and that under too turbulent conditions to disruption of particle/bubble aggregates. Teague and Lollback (2012) developed a rougher, cleaner, scavenger flotation scheme based on Jameson cells for beneficiation of phosphate ore feed slurry with up to 80 wt% particles finer than 20 μm to recover at least 80% phosphorus at a grade of 32% P_2O_5 or greater. However, their process requires slurry conditioning with reagents at high wt% solids (at least 70 wt%), use of guar gum as depressant and deionized water in addition to regular reagents such as soda ash, tall oil fatty acid and diesel and therefore the process may not be economically feasible. Liu et al (2017) found that saponified gutter oil fatty acid is an effective collector for reverse flotation of apatite from dolomite in collophaite ore. Zhou et al (2017) demonstrated in micro-flotation tests that use of reactive oily bubble can effectively enhance collophane flotation to produce superior separation performance. However, a practical and cost effective flotation approach has not been developed to increase the flotation recovery and reduce the flotation reagent consumption at the same time.

It is known that tiny nanobubbles or gas nuclei of less than 1 μm naturally exist in liquids such as seawater, distilled water, and blood (Johnson and Cooke 1981). It has been found (Schubert 2005, Hampton and Nguyen 2009) that nanobubbles accumulate preferentially at the hydrophobic solid–water interface, which has been confirmed by the atomic force microscopy (AFM) (Attard 2003, Mishchuk and Ralston 2006, Hampton and Nguyen 2010, Fan et al 2013, Li and Zhao 2014, Azevedo et al 2016, Knupfer et al 2017). Tiny nanobubbles attach more readily to particles than large bubbles due to their unique characteristics such as huge specific surface area, lower ascending velocity in water and rebound velocity from the surface, higher surface free energy to be satisfied, greater contact angle on solid surface, etc (Ducker 2009, Liu et al 2013, Calgaroto et al 2014, Azevedo et al 2016). Nanobubbles on particle surface activate flotation by promoting the attachment of larger bubbles since the attachment between nanobubbles and conventional sized bubbles is more favored than bubble/solid attachment. In other words, nanobubbles act as a secondary collector for particles, reducing flotation collector dosage, enhancing particle attachment probability and reducing the detachment probability. This leads to substantial improvement in flotation recovery of poorly floating phosphate particles and reduced reagent cost (Tao et al 2006, Fan and Tao 2008), which is one of the largest operating costs in commercial phosphate flotation plants. Application of nanobubbles to coal flotation resulted in an increase in flotation yield up to 15 wt%, a frother dose reduction of 10%, and a collector dose reduction of 90% (Attalla et al 2000). Similar results were obtained by Fan et al (2013). Calgaroto et al (2015) reported that use of nanobubbles (200 - 720 nm) improved the flotation recoveries of quartz fines and ultrafines by up to 20–30% and the higher contact angles and quartz fine aggregation in the presence of nanobubbles are claimed to be the most important mechanisms involved. Peng and Xiong (2015a, 2015b) confirmed that nanobubbles significantly increased coal flotation recovery.

This study was carried out to demonstrate the technical viability of the nanobubble flotation technology for the beneficiation of a plant phosphate flotation feed using a 5 cm in diameter flotation column featured with a static mixer to generate microbubbles and a cavitation tube to produce nanobubbles. Operating parameter examined in the study included feed flow rate, dosage of collector, dosage of frother, flotation time, etc.

2 Experimental

2.1 Flotation feed samples

The phosphate sample was collected from the conditioner feed streams in a Mosaic phosphate beneficiation plant in Florida, USA and placed in sealed containers. The phosphate samples were thoroughly mixed and split into small lots for storage in the lab. Representative samples were taken for size distribution analysis and chemical analysis.

2.2 Chemical analysis

XRD analyses of the phosphate flotation feed sample were conducted using Bruker D-8 Discover X-2 Advanced Diffraction Cabinet System equipped with Pelteir detector with stationary sample stage to identify principal elements. The XRD apparatus uses CuKa radiation source. The chemical composition of the phosphate samples was analyzed with the S4 PIONEER - wavelength dispersive X-ray fluorescence spectrometer (WDXRF). Up to 10 primary beam filters, 4 collimators, and 8 crystals can be utilized, which provides great analytical flexibility. The integrated standardless evaluation for all kind of samples like rocks, minerals, metals, hydrocarbons and industrial products allows the fast and easy determination of element concentrations from 100% down to the ppm-level without performing a calibration.

2.3 P_2O_5 content analysis

The P_2O_5 content analysis of phosphate sample was performed according to the standard procedure described by Zhang and Bogan (1994). About 1 gm of the dried and ground representative sample was digested in 50 ml of boiling aqua regia (a mixture of nitric and hydrochloric acids) on a hotplate until the reaction was complete. After

cooling, this solution was filtered through a Whatman 42 filter paper into a 1000 ml volumetric flask. The filter paper and residue were then washed at least five times to remove all traces of dissolved salts and acid. The filtrate was diluted with distilled water and thoroughly mixed. The concentrations were analyzed using an Inductively Coupled Plasma (ICP) emission spectrometer.

2.4 Acid insoluble analysis

Acid soluble components and acid insoluble components were analyzed using the industry's standard method described by Zhang and Bogan (1994). Acid-insoluble material was measured as an aqua-regia-insoluble material. Insoluble analysis was performed using the gravimetric method. Using a clean, tarred crucible, the filter paper and residue obtained from the digestion step was ignited at 900°C. After the crucible cooled, the acid insoluble in the sample was calculated.

2.5 Bubble size measurement

A Cillas 1064 laser particle size analyzer was used to measure the cavitation tube generated nanobubbles and the static mixer generated conventional sized bubbles. Details are provided elsewhere (Fan et al 2010).

2.6 Flotation reagents

The collector employed in the present study was a mixture of a fatty acid (FA-18G) and fuel oil at the ratio of 3:2 by weight. A glycol frother (F-507) was used to reduce water surface tension. Both frother and collector were obtained from the phosphate company. The collector dosage and frother dosage were fixed at 0.9 kg/ton and 10 ppm respectively. Soda ash was used as the pH modifier for the feed sample.

2.7 Laboratory flotation with phosphate samples

The specially designed flotation column shown in Figure 1

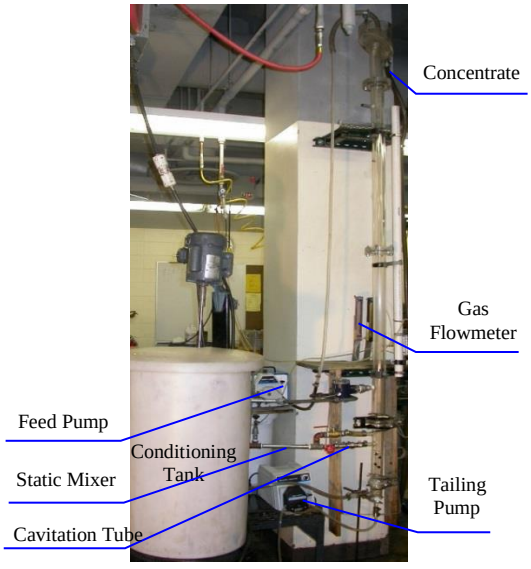

Figure 1 Specially designed flotation column

was used to perform flotation tests with phosphate samples. The column was made of Plexiglas of 5 cm in diameter and 1.8 m in height. The cavitation tube and the static mixer were used to generate nanobubbles and conventional sized bubbles, respectively.

The flotation procedure is briefly described as follows: 2 kg phosphate sample was employed to make flotation feed slurry for each run. Sodium hydroxide was used to adjust the pH between 9.1 and 9.5. The flotation feed was conditioned with the collector for 3 minutes at a predetermined solids concentration (75% solids unless otherwise specified) using a mechanical agitator. The conditioned phosphate sample was diluted to 25% solids content by weight and fed tangentially into the flotation column through a peristaltic pump, which allowed a consistent underflow stream. Phosphate slurry feed rate was 800 ml/min. A glycol frother (F-507) was used for the phosphate flotation tests. The total recycling flow rate for nanobubble and conventional sized bubble generation was maintained at 8.0 l/min.

3 Results and Discussion

Figure 2 shows the XRD intensity (cps, counts per second) versus XRD 2θ of the Mosaic phosphate sample. The amplitudes for specific XRD peaks indicate that the major mineral composition of the phosphates samples were quartz (SiO_2) and apatite ($Ca_5F(PO_4)_3$). The peak amplitudes for other minerals such as dolomite ($CaMg(CO_3)_2$), wavellite ($(AlOH)_3(PO_4)_2 \bullet 5H_2O$), Crandallite ($Ca_{0.7}Sr_{0.3}Al_3(PO_4)_2(OH)_5H_2O$), and K feldspar ($KALSi_3O_8$) etc. were very small, indicating that contents of these minerals in the phosphate samples are very low.

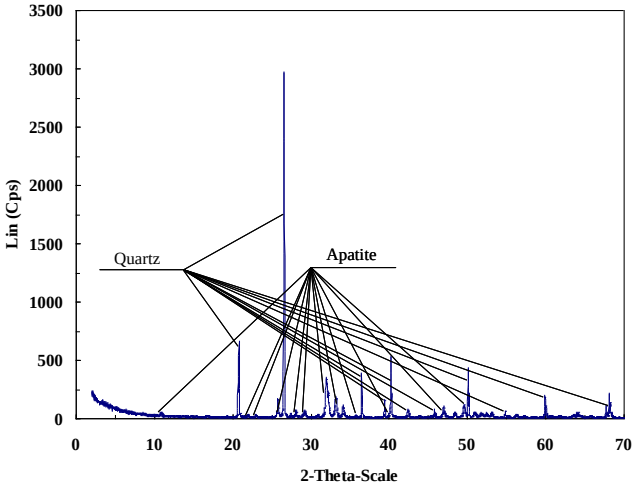

Figure 2 Mosaic phosphate XRD intensity cps versus 2θ

The particle size distribution results of the +100 mesh (>0.15 mm) phosphate plant flotation feed sample are shown in Figure 3. It was wet screened into eight size fractions. The curve of cumulative undersize against particle size shows that the median size of the phosphate sample was about 0.4 mm. Most particles or about 80% were coarser than 50 mesh or 0.3 mm. Less than 2% particles were

smaller than 100 mesh or 0.15 mm and less than 1% particles were larger than 16 mesh or 1.18 mm. It should be noted that the flotation feed was the phosphate sample deslimed at 100 mesh to remove high concentrations of clays, which is the standard practice in the Florida phosphate industry. In other words, the lab flotation feed sample was the same as the plant flotation feed sample. The phosphate sample contained 15.6% moisture, 10.16% P_2O_5, and 67.23% Acid Insoluble (A.I.).

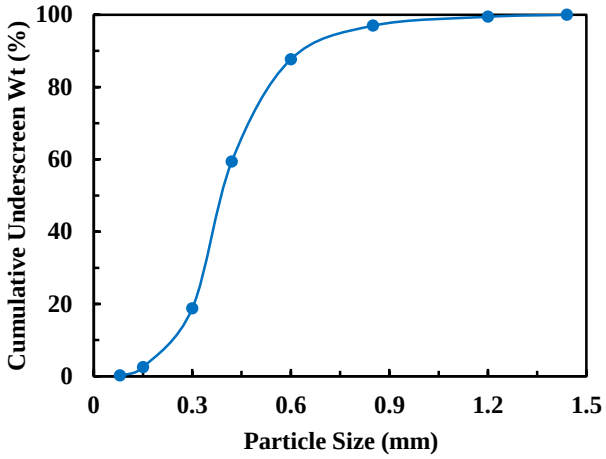

Figure 3 Phosphate particle size distribution

Figure 4 shows the size distribution of bubbles generated by the cavitation tube and static mixer at a frother dosage of 10 ppm. There are two major distribution peaks observed on the population frequency curve. They represent nanobubbles with a d_{50} of approximately 830 nm and micro-size bubbles with an average of about 70 μm generated by the cavitation tube and the static mixer, respectively. Obviously, the nanobubbles are approximately two orders of magnitude smaller than microbubbles and this result is consistent with other studies (Peng and Xiong 2015a, 2015b). Oliveira et al (2018) reported that even smaller nanobubbles (230-280 nm) can be generated with a cavitation tube and the size of nanobubbles depends on liquid surface tension, air/liquid ratio, etc. Etchepare et al (2017) used a multiphase pump and a needle valve to generate 150-220 nm nanobubbles with a concentration of up to 4×10^9 nanobubbles ml^{-1}. They found that nanobubbles were highly stable and resistant to shearing caused by pump impellers and to high operating pressures (up to 5 bar).

Figure 5 shows the effect of feed rate on concentrate grade and flotation recovery without nanobubbles. It can be observed from Figure 5 that the P_2O_5 recovery decreased from about 87% to 57% as the feed rate increased from 120 g/min to 600 g/min. This was a result of decreased flotation time with feed rate increasing. The P_2O_5 content in the concentrate increased slightly from about 26.5% to 27.5% as the feed rate increased whereas A.I. content decreased from 22.8% to 19.1%.

Figure 6 shows the effect of feed rate on flotation recovery and concentrate grade with nanobubbles. It can be observed that the P_2O_5 recovery decreased only slightly from 98% to about 96.5% as the feed rate increased from 120 g/min to 360 g/min. When the feed rate increased from 360 g/min to 600 g/min, the P_2O_5 recovery decreased to 77%. The P_2O_5 in the concentrate increased from 28.5% to 29.0% as the feed rate increased. Comparing Figure 6 with Figure 5 clearly indicates that use of nanobubbles not only increased P_2O_5 recovery but also improved concentrate grade, suggesting flotation separation efficiency was remarkably enhanced in the presence of nanobubbles.

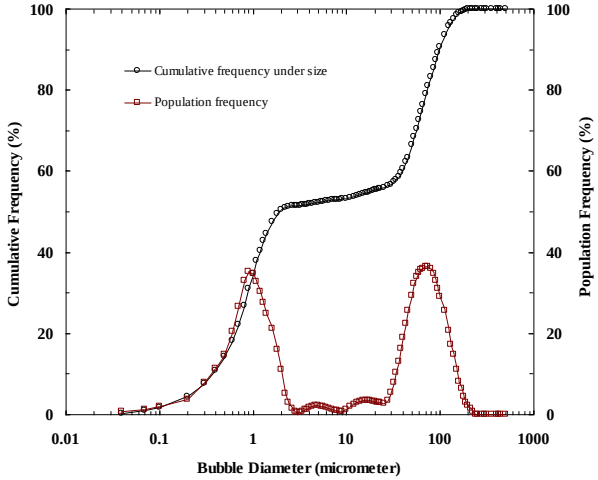

Figure 4 Size distribution of cavitation tube and static mixer generated bubbles

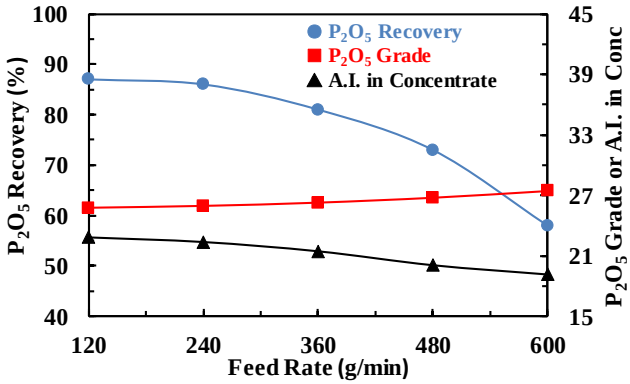

Figure 5 Effect of feed rate on concentrate grade and recovery without nanobubbles

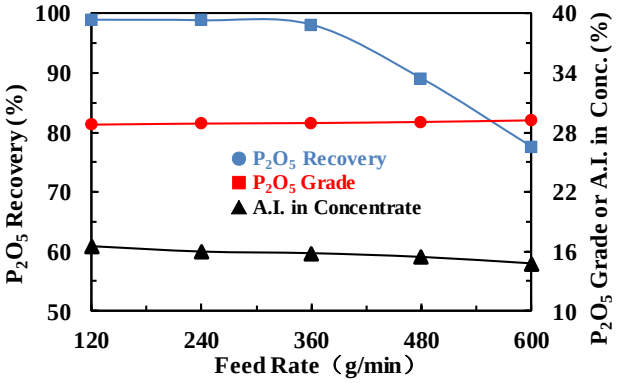

Figure 6 Effect of feed rate on concentrate grade and recovery with nanobubbles

Figure 7 shows the flotation separation efficiency curve based on the relationship between the A.I. rejection and P_2O_5 recovery obtained under the different feed rates with and without nanobubbles. The remarkable differences in two separation curves clearly indicate that the use of nanobubbles significantly enhanced the separation efficiency of froth flotation. Nanobubbles always produced a higher P_2O_5 recovery at a given A.I. rejection. For example, P_2O_5 recovery was about 30% higher at an A.I. rejection of 80%. The improvement in flotation separation efficiency by nanobubbles can be attributed to the selectivity of nanobubbles for hydrophobic particles previously demonstrated by other investigators (Hampton and Nguyen 2010, Fan et al 2013, Sobhy and Tao 2013a, Li and Zhao 2014, Azevedo et al 2016, Knupfer et al 2017). Similar flotation efficiency improvements by nanobubbles with other minerals have been reported by others (Sobhy and Tao 2013a, 2013b, Calgaroto et al 2015, Peng and Xiong 2015a, 2015b).

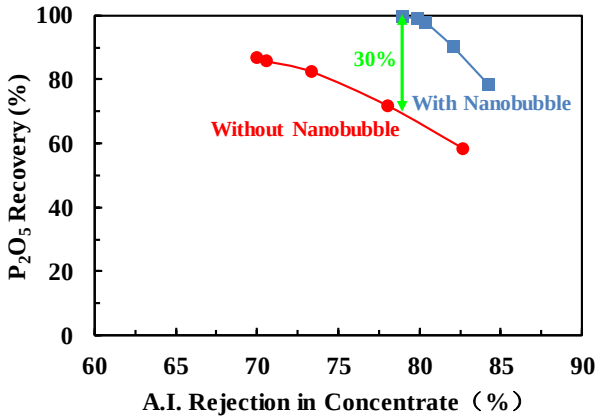

Figure 7 Effects of nanobubbles on separation efficiency curve

Figure 8 shows the effects of nanobubbles on flotation concentrate P_2O_5 recovery and grade at different collector dosages varying from 0.3 kg/ton to 2.1 kg/ton. It should be pointed out that there were no noticeable differences in the product grade with or without nanobubbles and therefore only one grade curve is shown in Figure 8. In these tests, the flotation feed rate, superficial air velocity, and frother dosage were fixed constant at 240 g/min, 1.0 cm/s, and 10 ppm, respectively. The curves in the figure indicate that the P_2O_5 flotation recovery increased remarkably as the collector dosage increased from a dosage of 0.3 kg/ton to 0.9 kg/ton with or without nanobubbles. The P_2O_5 recovery increased slightly in the absence of nanobubbles while the P_2O_5 recovery remained essentially constant in the presence of nanobubbles as the collector dosage increased from 0.9 kg/ton to 2.1 kg/ton. The maximum flotation recovery of approximately 98% and a concentrate grade of 28.8% were achieved at a collector dosage of 0.9 kg/t in the presence of nanobubbles. In contrast, the maximum flotation recovery of less than 94% was achieved at a collector dosage of 2.1 kg/t in the absence of nanobubbles. In other words, a higher maximum recovery was achieved with less collector in the presence of nanobubbles, suggesting use of nanobubbles increased P_2O_5 recovery and reduced required collector dosage. In this particular case, the required collector dosage was reduced from 2.1 kg/t to 0.9 kg/t by the introduction of nanobubbles, representing a collector cost saving of more than 50%.

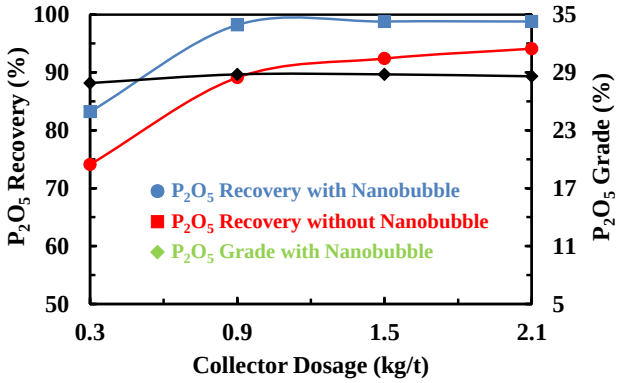

Figure 8 Effects of nanobubbles on P_2O_5 recovery and grade at different collector dosages

Figure 9 shows the effects of nanobubbles on flotation P_2O_5 recovery at varying frother dosages from 0 to 20 ppm. There were no noticeable differences in the product grade (P_2O_5% or A.I.%) in the presence and absence of nanobubbles and thus the grade data is not shown in Figure 9 for the purpose of clarity. The curves indicate that nanobubbles improved P_2O_5 recovery at lower frother dosage more significantly than at higher frother dosages. The flotation P_2O_5 recovery increased remarkably as the frother dosage increased from a dosage of 0 to 10 ppm. The flotation P_2O_5 recovery increased slightly in the absence of nanobubbles while the flotation P_2O_5 recovery remained essentially constant in the presence of nanobubbles as the frother dosage increased from a dosage of 10 ppm to 20 ppm. The flotation recovery of more than 98% and a concentrate grade of 28.8% were achieved at a frother dosage of 10 ppm in the presence of nanobubbles. By comparison, the maximum flotation recovery was 96% in the absence of nanobubbles, which was achieved at a frother dosage of 20 ppm.

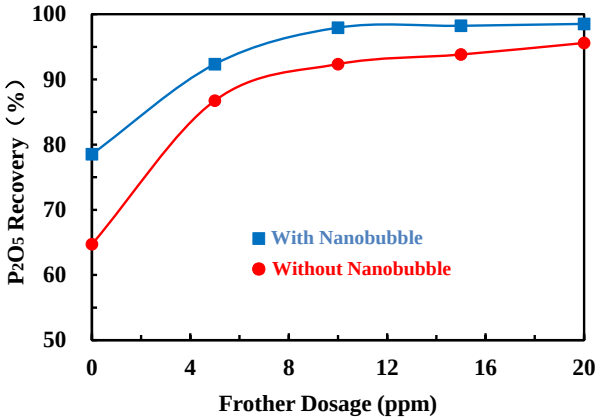

Figure 9 Effects of nanobubbles on P_2O_5 recovery at different frother dosages

The results shown in Figure 9 clearly indicate that use of nanobubbles reduced the required frother dosage by 50% and increased flotation recovery at the same time. It should be noted that reagent expense is one of the biggest cost items for a mineral processing plant and a reduction of 50% in both the collector and frother dosage represents a major economic benefit.

Figure 10 shows the effect of nanobubbles on flotation kinetics expressed as the P_2O_5 recovery vs. flotation time curve for the +0.425-1.18 mm particle size fraction. The differences in curves with and without nanobubbles suggest that the P_2O_5 recovery in the presence of nanobubbles was significantly higher at a given flotation than in the absence of nanobubbles. For example, when the flotation time was 1 minute, the P_2O_5 recovery in the presence of nanobubbles was about 21% higher than in the absence of nanobubbles. The results reveal that the presence of nanobubbles improved flotation kinetics. Based on the flotation recovery in the first minute it can be approximated that the first order flotation rate constant k is 1.89 min^{-1} and 1.01 min^{-1} with and without nanobubbles, respectively. It should be pointed out that similar improvements in flotation kinetics were observed with all other size fractions such as 0.425-0.60 mm, 0.6-0.85 mm, 0.85-1.18 mm fractions. The improvement in flotation kinetics observed in this study is consistent with previous findings (Hampton and Nguyen 2010, Calgaroto et al 2014, Calgaroto et al 2015, Ahmadi et al 2014, Zhou et al 2016) that nanobubbles are formed and attached more selectively and strongly on hydrophobic particles than conventional sized bubbles and also act as secondary collector to enhance surface hydrophobicity of mineral particles.

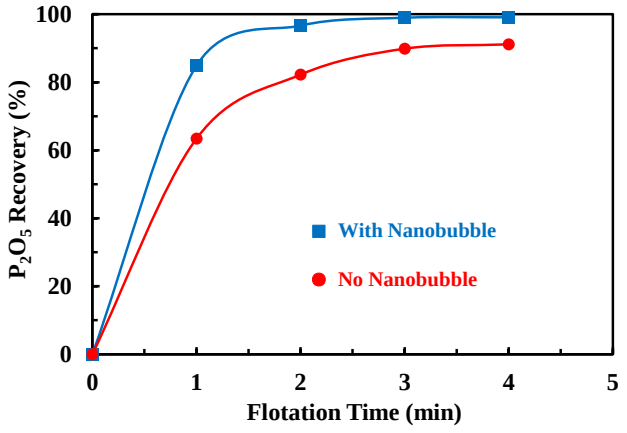

Figure 10 P_2O_5 Recovery as a function of flotation time for +0.425-1.18 mm size fraction of phosphate

4 Results and Discussion

Based on the above data and discussion, the following conclusions can be drawn:

(1) The median size of cavitation tube generated nanobubbles was about 830 nm, which was approximately two orders of magnitude smaller than microbubbles generated by the static mixer.

(2) Laboratory column flotation results show that use of nanobubbles significantly improved phosphate flotation performance. The separation performance curves obtained at different feed rates indicate that phosphate recovery can be increased by as much as 30% at a given concentrate grade.

(3) The flotation recovery of 98% was achieved at a collector dosage of 0.9 kg/t in the presence of nanobubbles at a concentrate grade of 28.79% P_2O_5. In contrast, the maximum flotation recovery of 94% was obtained at a collector dosage of 2.1 kg/t in the absence of nanobubbles. In other words, nanobubbles increased P_2O_5 recovery by 4% and reduced collector dosage by more than 50% at the same time. Similar results were observed with frother dosage which was reduced by 50% in the presence of nanobubbles.

(4) Size-by-size flotation test results indicated that nanobubbles improved the first order flotation rate constant k from 1.01 min^{-1} to 1.89 min^{-1} for the +0.425-1.18 mm size fraction of phosphate particles . Similar improvements were observed with all particle size fractions.

(5) The improvement in phosphate flotation performance can be attributed to the enhanced collection efficiency and increased surface hydrophobicity of phosphate particles as a result of unique characteristics of nanobubbles.

Acknowledgement

The authors would sincerely acknowledge the financial support provided by the Florida Industrial and Phosphate Research (FIPR) Institute through a project numbered FIPR 05-02-172R which made this work possible. The project manager Dr. Patrick Zhang's valuable advice and professional guidance is deeply appreciated.

References

Ahmadi, R., D.A. Khodadadi, M. Abdollahy and M. Fan, 2014. Nano-microbubble flotation of fine and ultrafine chalcopyrite particles. International Journal of Mining Science and Technology, **24**: 559 - 566.

Attard, P., 2003. Nanobubbles and the hydrophobic attraction. Advanced Colloid Interface Science, **104** (**1-3**): 75 - 95.

Azevedo, A., R. Etchepare, S. Calgaroto and J. Rubio, 2016. Aqueous dispersions of nanobubbles: generation, properties and features. Minerals Engineering, **94**: 29 - 37.

Calgaroto, S., K.Q. Wilberg and J. Rubio, 2014. On the nanobubbles interfacial properties and future applications in flotation. Minerals Engineering, **60**: 33 - 40.

Calgaroto, S., A. Azevedo and J. Rubio, 2015. Flotation of quartz particles assisted by nanobubbles. International Journal of Mineral Processing, **137**: 64 - 70.

Calle-Castañeda, S.M., M.A. Márquez-Godoya and J.P. Hernández-Ortiza, 2018. Phosphorus recovery from high concentrations of low-grade phosphate rocks using the biogenic acid produced by the acidophilic bacteria Acidithiobacillus thiooxidans. Minerals Engineering, **115**: 97 - 105.

Davis, B.E. and G.D. Hood, 1993. Improved recovery of coarse Florida phosphate. Mining Engineering, **45**(**6**): 596 - 599.

Ducker, W.A., 2009. Contact angle and stability of interfacial nanobubbles. Langmuir, **25**(**16**): 8907 - 8910.

Etchepare, R., H. Oliveira, M. Nicknig, A. Azevedo and J. Rubio, 2017. Nanobubbles generation using a multiphase pump, properties and features in flotation. Minerals Engineering, **112**: 19 - 26.

Fan, M. and D. Tao, 2008. Effect of picobubbles by hydrodynamic cavitation on coarse phosphate froth flotation. XXIV International Mineral Processing Congress, Beijing, China. (in Chinese)

Fan, M., D. Tao and Z. Luo, 2010. Nanobubble generation and its application in froth flotation (part I): nanobubble generation and its effects on properties of microbubble and millimeter scale bubble solutions. Mining Science and Technology, **20**(**1**): 1 - 19.

Fan, M., D. Tao, Y. Zhao and R. Honaker, 2013. Effect of nanobubbles on the flotation of different sizes of coal particle. Minerals and Metallurgical Processing. **30**(**3**): 157 - 161.

Hampton, M.A. and A.V. Nguyen, 2009. Accumulation of dissolved gases at hydrophobic surfaces in water and sodium chloride solutions: implications for coal flotation. Minerals Engineering, **22** (**9**-**10**): 786 - 792.

Hampton, M.A. and A.V. Nguyen, 2010. Nanobubbles and the nanobubble bridging capillary force. Advanced Colloid Interface Science, **154** (**1**/**2**): 30 - 55.

Johnson, B.D. and R.C. Cooke, 1981. Generation of stabilized microbubbles in seawater. Science, **213**: 209 - 211.

Knupfer, P., L. Ditscherlein and U.A. Peuker, 2017. Nanobubble enhanced agglomeration of hydrophobic powders. Colloids and Surfaces A, **530**: 117 - 123.

Li, D. and X. Zhao, 2014. Micro and nano bubbles on polystyrene film/water interface. Colloids and Surfaces A: Physicochemical and Engineering Aspects, **459**: 128 - 135.

Liu, S., Y. Kawagoe, Y. Makino and S. Oshita, 2013. Effects of nanobubbles on the physicochemical properties of water: the basis for peculiar properties of water containing nanobubbles. Chemical Engineering Science, **93**: 250 - 256.

Liu, X., C. Li, H. Luo, R. Cheng and F. Liu, 2017. Selective reverse flotation of apatite from dolomite in collophanite ore using saponified gutter oil fatty acid as a collector. International Journal of Mineral Processing, **165**: 20 - 27.

Maksimov, I.I., L.A. Otrozhdennova, A.D. Borkin, M.F. Yemelyanov and L.A. Nechay, 1993. An investigation to increase the efficiency of coarse and fine particle flotation in ore processing of non-ferrous metals. In: Proceedings of XVIII International Mineral Processing Congress, pp. 685 - 687.

Mendes, G., A.M. de Freitas, O.L. Pereira, I. Silva, N. Vassilev and M.D. Costa, 2014. Mechanisms of phosphate solubilization by fungal isolates when exposed to different P sources. Annuals of Microbiology, **64**(**1**): 239 - 249.

Mishchuk, N. and J. Ralston, 2006. Influence of very small bubbles on particle/bubble heterocoagulation. Journal of Colloid and Interface Science, **30**(**1**): 168 - 175.

Moudgil, B.M., 1992. Enhanced recovery of coarse particles during phosphate flotation. Final Report to Florida Institute of Phosphate Research, No. 02-067-099.

Oliveira, H., A. Azevedo and J. Rubio, 2018. Nanobubbles generation in a high-rate hydrodynamic cavitation tube. Minerals Engineering, **116**: 32 - 34.

Peng, F.F. and Y. Xiong, 2015a. Pico-nano bubble column flotation using static mixer-venturi tube for Pittsburgh No. 8 coal seam. International Journal of Mining Science and Technology, **25**(**3**): 347 - 354.

Peng, F.F. and Y. Xiong, 2015b. Optimization of cavitation venturi tube design for pico and nano bubbles generation. International Journal of Mining Science and Technology, **25**(**4**): 523 - 529.

Priha, O., T. Sarlin, P. Blomberg, L. Wendling, J. Mäkinen, M. Arnold and P. Kinnunen, 2014. Bioleaching phosphorus from fluorapatites with acidophilic bacteria. Hydrometallurgy, **150**: 269 - 275.

Ralston, J. and S.S. Dukhin, 1999. The interaction between particles and bubbles. Colloids and Surfaces, **151**: 3 - 14.

Rodrigues, W.J., L.S. Leal Filho and E.A. Masini, 2001. Hydrodynamic dimensionless parameters and their influence on flotation performance of coarse particles. Minerals Engineering, **14**(**9**): 1047 - 1054.

Schubert, H., 2005. Nanobubbles, hydrophobic effect, heterocoagulation and hydrodynamics in flotation. International Journal of Mineral Processing, **78**: 11 - 21.

Sis, H. and S. Chander, 2003. Reagents used in the flotation of phosphate ores: a critical review. Minerals Engineering, **16**: 577 - 585.

Sobhy, A. and D. Tao, 2013a. Nanobubble column flotation of fine coal particles and associated fundamentals. International Journal of Mineral Processing, **124**: 109 - 116.

Sobhy, A. and D. Tao, 2013b. High-efficiency nanobubble coal flotation. International Journal of Coal Preparation and Utilization, **33**(**5**): 242 - 256.

Tao, D., 2004. Role of bubble size in flotation of coarse and fine particles—A Review. Separation Science and Technology, **39**(**4**): 741 - 760.

Tao, D., M. Fan and B.K. Parekh, 2006. Picobubble enhanced flotation of coarse phosphate particles. Proceedings, XXIII International Mineral Processing Congress, Istanbul, Turkey.

Teague, A.J. and M.C. Lollback, 2012. The beneficiation of ultrafine phosphate. Minerals Engineering, **27**-**28**: 52 - 59.

Van Kauwenbergh, S., 2010. World phosphate reserves and resources. Fertilizer Outlook and Technology Conference. International Fertilizers Development Center (IFDC). Muscle Shoals. Al 35662 USA.

Yoon, R.H., 2000. The role of hydrodynamic and surface forces in bubble-particle interaction. International Journal of Mineral Processing, **58**: 128 - 143.

Zhang, P. and M. Bogan, 1994. Recovery of phosphate from Florida beneficiation slimes. Minerals Engineering, **8**: 523 - 34.

Zhou, W., L. Ou, Q. Shi and H. Chen, 2016. Aggregation of ultra-fine scheelite particles induced by hydrodynamic cavitation. International Journal of Mineral Processing, **157**: 236 - 240.

Zhou, F., L. Wang, Z. Xu, Y. Ruan and R. Chi, 2017. A study on novel reactive oily bubble technology enhanced collophane flotation. International Journal of Mineral Processing, **169**: 85 - 90.